WILLIAM & MARY
CHARTERED 1693

W&M ScholarWorks

VIMS Articles

Virginia Institute of Marine Science

Form and function of the bulbus arteriosus in yellowfin tuna (Thunnus albacares), bigeye tuna (Thunnus obesus) and blue marlin (Makaira nigricans): static properties

M H. Braun

Richard Brill
Virginia Institute of Marine Science, rbrill@vims.edu

J M. Gosline

D R. Jones

Follow this and additional works at: https://scholarworks.wm.edu/vimsarticles

Part of the Aquaculture and Fisheries Commons

Form and function of the bulbus arteriosus in yellowfin tuna (*Thunnus albacares*), bigeye tuna (*Thunnus obesus*) and blue marlin (*Makaira nigricans*): static properties

Marvin H. Braun[1,*], Richard W. Brill[2], John M. Gosline[3] and David R. Jones[4]

[1]*Department of Zoology, Cambridge University, Downing Street, Cambridge, UK, CB2 3EJ*, [2]*Cooperative Marine Education and Research Program, Virginia Institute of Marine Science, PO Box 1208, Great Rd, Gloucester Point, Virginia 23062, USA*, [3]*Department of Zoology, University of British Columbia, Vancouver, BC, Canada, V6T 1Z4* and [4]*Zoology Animal Care, 6199 South Campus Road, University of British Columbia, Vancouver, BC, Canada, V6T 1W5*

*Author for correspondence (e-mail: mhb31@cam.ac.uk)

Summary

The juxtaposition of heart and gills in teleost fish means that the Windkessel function characteristic of the whole mammalian arterial tree has to be subserved by the extremely short ventral aorta and bulbus arteriosus. Over the functional pressure range, arteries from blue marlin (*Makaira nigricans*) and yellowfin tuna (*Thunnus albacares*) have J-shaped pressure–volume (P-V) loops, while bulbi from the same species have r-shaped P-V loops, with a steep initial rise followed by a compliant plateau phase. The steep initial rise in pressure is due to the geometry of the lumen. The interactions between radius, pressure and tension require a large initial pressure to open the bulbar lumen for flow. The plateau is due to the unique organization of the bulbar wall. The large elastin:collagen ratio, limited amount of collagen arranged cirumferentially, lack of elastin lamellae and low hydrophobicity of the elastin itself all combine to lower stiffness, increase extensibility and allow efficient recoil. Even though the modulus of bulbus material is much lower than that of an artery, at large volumes the overall stiffness of the bulbus increases rapidly. The morphological features that give rise to the special inflation characteristics of the bulbus help to extend flow and maintain pressure during diastole.

Key words: bulbus arteriosus, P-V loop, r-shaped curve, stress, modulus, tuna, marlin, *Thunnus*, *Makaira*.

Introduction

The teleost bulbus arteriosus is located within the pericardial cavity and lies rostral to the ventricle. Typically, it is swollen proximally, tapering distally into the ventral aorta. Within these parameters, a large variety of shapes occur, but the functional significance of the different shapes is unknown (Santer, 1985). The internal morphology of the bulbus also shows a large amount of variance between species. The lumen can be smooth, ridged or trabeculated. The trabeculae can be 'spongy' or separated into discrete longitudinal and radial elements. Exceptionally, in one species of deep-sea *Macrouridae*, the proximal portion of the lumen contains a cartilaginous inner tube separate from the outer, spongy trabeculae (Greer-Walker et al., 1985). Unlike the rest of the heart (sinus venosus, atrium and ventricle), the bulbus arteriosus contains no cardiac muscle and is not actively contractile.

Whether the bulbus is cardiac or arterial in nature is an open question (Benjamin et al., 1983). However, due to some obvious similarities, arterial nomenclature is used to describe the bulbar morphology. As in arteries, the bulbar wall is composed of three layers: an intima composed of a single layer of endothelial cells, a thick media primarily composed of elastin and smooth muscle, and a collagenous adventitia surrounded by an outer layer of mesothelial cells.

The endothelial cells can be squamous, columnar or cuboidal (Leknes, 1981, 1985; Benjamin et al., 1983, 1984) and often contain membrane-bound bodies that stain strongly with periodic acid-Shiff's, indicating the presence of carbohydrates (Benjamin et al., 1983; Leknes, 1981). There is microscopic evidence for the discharge of membrane-bound vesicles into the lumen (Benjamin et al., 1983); however, their contents are unknown. Except for the layer of mesothelial cells, the adventitia is almost entirely collagen (Benjamin et al., 1983; Bushnell et al., 1992) and is thought to limit bulbar strain (Priede, 1976; Raso, 1993; Icardo et al., 1999a,b). The media forms 90–95% of the bulbus and is composed of smooth muscle sparsely distributed within an elastin framework (Licht and Harris, 1973; Watson and Cobb, 1979; Icardo et al., 2000). Exceptions do exist, however, as the bulbus of *Pleuronectes platessa* contains no smooth muscle (Santer and Cobb, 1972).

The term 'J-shaped curve' is used to describe the non-linear mechanical properties (stress and modulus) of biological materials. While arterial P-V loops are often sigmoidal, the non-linear transformation of pressure into stress, and volume into strain, results in J-shaped stress–strain curves. Furthermore, over the operational pressure range, most arterial P-V curves are J-shaped. Within arteries, the J-shaped curve results from elastin and collagen working in conjunction as a strain-limiting system (Wainwright et al., 1976). At low extensions, rubber-like elastin resists deformation, resulting in a low initial slope. However, at higher extensions, the collagen in the arterial wall (approximately $1000\times$ stiffer than elastin) is also recruited to resist deformation, increasing the stiffness of the arterial wall and causing a sharp increase in the slope. Bulbi also possess elastin, smooth muscle and collagen, but when a bulbus is inflated (Licht and Harris, 1973; Priede, 1976; Bushnell et al., 1992) the P-V loops can best be described as 'r-shaped' over the physiological pressures, with the distinguishing feature being a continuously decreasing slope. With respect to the bulbar inflations, the r-shaped curve describes a sharp initial rise in pressure followed by a plateau phase in which large changes in volume result in small changes in pressure.

While both the cause and the significance of the J-shaped arterial P-V loop have been studied extensively and are well understood, similar studies of the unique bulbar inflations do not exist, leaving a fundamental piece of fish physiology unknown. To this end, the analysis presented here addresses the causes of the r-shaped bulbar P-V curve and relates the mechanical properties of the wall material to the many modifications that have occurred within the bulbar wall.

Materials and methods

Gross morphology and histology

Bulbi from blue marlin (*Makaira nigricans* L.) and yellowfin tuna (*Thunnus albacares* L.) were obtained from fish sold at the Honolulu fish auction (Honolulu, HI, USA). We estimate the fish were brought to auction up to 72 h after capture, resulting in possible smooth muscle death. Despite the delay, few histological changes occurred, as the fish were always kept carefully chilled to prevent tissue deterioration before sale.

The gross morphology of the bulbi was compared between species and pictures were taken. Two bulbi and ventral aortae from yellowfin tuna were fixed in buffered formalin and sent to Wax-it Histology Services (Aldergrove, BC, Canada) for sectioning and staining. One bulbus was fixed at physiological pressure (10 kPa), while the other was fixed at zero pressure. The sections were stained with a Verhoeff's elastic stain.

Yellowfin tuna bulbi for use in electron microscopy were prefixed in buffered formalin to prevent structural changes while the tissues were transported to the University of British Columbia Electron Microscopy Facility (Vancouver, BC, Canada). Samples were fixed in 2.5% glutaraldehyde in 0.1 mol l^{-1} sodium cacodylate (pH 7.2) and, following fixation, were washed in 0.1 mol l^{-1} sodium cacodylate buffer overnight and post-fixed in 1% osmium tetroxide. After a graded alcohol dehydration, the samples were stained using uranyl acetate and lead and embedded in Epon/Araldite. The blocks were sectioned with a glass knife and viewed with a Zeiss EM 10C (Carl Zeiss Inc., Oberkochen, Germany).

P-V loops

Bulbi from small yellowfin tuna (<3 kg) were obtained from freshly killed fish held in large outdoor tanks at the National Marine Fisheries Service Kewalo Research Facility in Honolulu, HI, USA. The water temperature in the holding tanks was 25°C. After death, an incision slightly posterior to the gills was made on the ventral surface, exposing the pericardium. The pericardium was slit in the midline, and the length of the bulbus arteriosus was measured *in situ*. The bulbus arteriosus was then removed by cutting posterior to the bulbo-ventricular junction and anterior to the bulbo-aortic junction and placed in saline. Bulbi from larger yellowfin tuna (>10 kg) and blue marlin (>25 kg) came from the fish auction in Honolulu and were removed through a lateral incision underneath the operculum.

Sections of blue marlin ventral aortae were dissected from fish being sold at the Honolulu fish auction, while yellowfin tuna ventral aortae were dissected from freshly killed animals. All yellowfin tuna dorsal aortae were inflated *in situ* as they are tightly bound to the spinal column and our attempts to separate them resulted in leaks. For two yellowfin tuna, the dorsal aortae were heavily parasitized by the larval cestode *Dasrhynchus talismani* (Brill et al., 1987).

The bulbus was double cannulated using PE tubing with flared ends, and ligatures were placed behind the flare around the bulbo-ventricular and bulbo-arterial junctions. The anterior cannula was attached to a pressure transducer, while the posterior cannula was attached to a syringe filled with saline solution. The bulbi from yellowfin tuna were held in a tissue bath at their *in vivo* length. The blue marlin bulbi were not held at any specific lengths because we were unable to measure their *in vivo* size during removal through the lateral incision. The sizes of tubing or syringes were picked to best fit the size of the bulbus. We chose tubing that approximated the diameter of the ventral aorta and syringes that were determined experimentally to be 150% of the respective bulbar volume. The saline solution was left at room temperature (25°C). The arteries were also cannulated in both ends, with one cannula attached to a pressure transducer and the other to an infusion syringe.

A measured volume of fluid was then injected into the bulbus or artery in steps, and the resultant pressure signal was amplified and recorded using DASYLAB software (Dasytec USA, Amherst, NH, USA). To limit the effects of stress–relaxation, cycles of inflation and deflation were performed until consistent results were seen. Preconditioning usually required 5–10 cycles for the bulbus and 3–5 cycles for the arteries. These initial cycles were discarded. Each experiment consisted of 8–15 trials, and results from any trials in which a loss of more than 5% of the injected saline occurred were not used.

Stress (σ) was expressed as true stress and was calculated assuming constant volume as:

$$\sigma = (1 + \varepsilon_c)\mathbf{F}/a_0 , \qquad (2)$$

where $\mathbf{F}$ is measured force, a_0 is the initial cross-sectional area and ε_c is the mean value of strain over which the stress has been calculated.

For bulbar loops, we used a value of thickness that was smaller than the full thickness of the bulbus wall to calculate stress because in a number of force–extension studies, the inner medial layer of the bulbus (with longitudinal elastin fibres) ripped with no change in the slope of the force curve being generated. This suggested that the inner layer of the bulbus was contributing little circumferential strength to the wall. Consequently, including the thickness of the inner medial layer when calculating stress would result in a significant underestimation of the true stress. The inner media is approximately 60% of the wall and, therefore, the value used was approximately 40% of the full thickness of the bulbus wall.

Circumferential stiffness was calculated, according to Bergel (1961), as the incremental modulus (E_{inc}):

$$E_{inc} = (1 - \nu^2)\Delta\sigma/\Delta\varepsilon_c , \qquad (3)$$

where ν is Poisson's ratio for the artery or bulbus. Poisson's ratio is the negative quotient of circumferential strain and longitudinal strain. In most soft tissues, Poisson's ratio is near 0.5 (Bergel, 1961) and, for the purposes of our calculations, we accepted this value.

The stress–strain curves were smoothed using TABLECURVE (Jandel Scientific, San Rafael, CA, USA), a curve-fitting program that generates a number of different equations describing the curve. Once an appropriate fit was found, the equation was used to generate the exact dependent value of any desired independent variable (the y-value for any input x). This allowed the comparison of different stress–strain curves at the same values of strain.

Statistics

Descriptive statistics (means ± S.E.M.) were calculated for the P-V curves generated by blocking the smooth muscle and heating the bulbus, as well as for all the stress–strain curves generated by the various extension protocols. The treatments in the blocking and heating study were compared using a two-way repeated measures analysis of variance (ANOVA). For comparisons between the stress–strain curves for the anterior, middle and posterior segments of the tuna and marlin bulbi, a two-way ANOVA was performed. Multiple comparisons between the different treatments for the P-V and stress–strain curves were performed using a Tukey test. All comparisons between groups were performed using SIGMASTAT 2.0 (Jandel Scientific).

Results
Gross morphology and histology

The bulbus arteriosus of the yellowfin tuna is largest proximal to the heart, tapering down towards the ventral aorta (Fig. 1A). Internally, it possesses a complex array of longitudinal elements: elastic chords that arise from the ventricular end as discrete structures and are much more securely attached to the lumen wall near the ventral aorta, becoming ridges (Fig. 1B). The longitudinal elements often radiate out from locations near the bulbo-ventricular pocket valves. Compared with the bulbus arteriosus of the yellowfin tuna, the bulbus of the blue marlin is much longer and thinner walled (Fig. 1C). Many of the internal longitudinal elements are attached to the bottom of the bulbo-ventricular pocket valves (Fig. 1D).

There are obvious differences between cross-sections from a yellowfin tuna bulbus (Fig. 2A) and ventral aorta (Fig. 2B). Despite the fact that these sections were separated by <1 cm, they show a large difference in wall thickness. It is within the wall, however, where the important differences occur. The ventral aorta has a typical arterial composition. Layers of smooth muscle (sm), sheets of elastin called lamellae (el) and collagen (co) are found in close proximity, forming regular layers throughout the wall. By contrast, the anterior bulbus of yellowfin tuna contains no elastin lamellae. The elastin fibres (ef) are ordered but not joined into large continuous sheets. In the ventral aorta, elastin lamellae alternate with layers of smooth muscle. Despite the same staining technique, no smooth muscle is obvious in this bulbus section (Fig. 2A).

Bulbar elastin is stained very heavily with Verhoeff's elastin stain, obscuring much of the smooth muscle. Despite this, layers of smooth muscle can still be seen. Fig. 2C is a longitudinal section of the bulbus near the ventricle and shows a block of smooth muscle that is sandwiched between two layers of longitudinal elastin fibres (lf). The smooth muscle layer extends anteriorly just beyond the top of the frame in Fig. 2D and posteriorly until it appears to attach to the collagenous ventriculo-bulbar pocket valve.

The adventitia (a) of the yellowfin bulbar wall is a thin fibrous layer (Fig. 3A,B) containing mesothelial cells and collagen. The bulk of the bulbar collagen is concentrated in this outer layer. The adventitia does contain a small amount of elastin; however, it is not as ordered or in as high a concentration as in the rest of the bulbus. The majority of the bulbus wall is media (m), which is divided into two layers: a dense outer layer containing elastin fibres running in a circumferential manner (om) and a 'looser' inner media in which the majority of the elastin fibres are oriented longitudinally (im; Fig. 3A,B). This inner media contains the longitudinal elements (le).

Wall thickness and internal morphology differ throughout the length of the bulbus. While the size of the collagenous adventitia remains relatively constant in both sections, the outer media at the posterior end (Fig. 3B) is approximately half the thickness of the same layer in the middle bulbus (Fig. 3A). This is accompanied by an increase in the size and complexity of the inner media, specifically the longitudinal elements. The architecture of the longitudinal elements is most elaborate near the ventricle. Their morphology is very irregular, with an overall 'spongy' appearance.

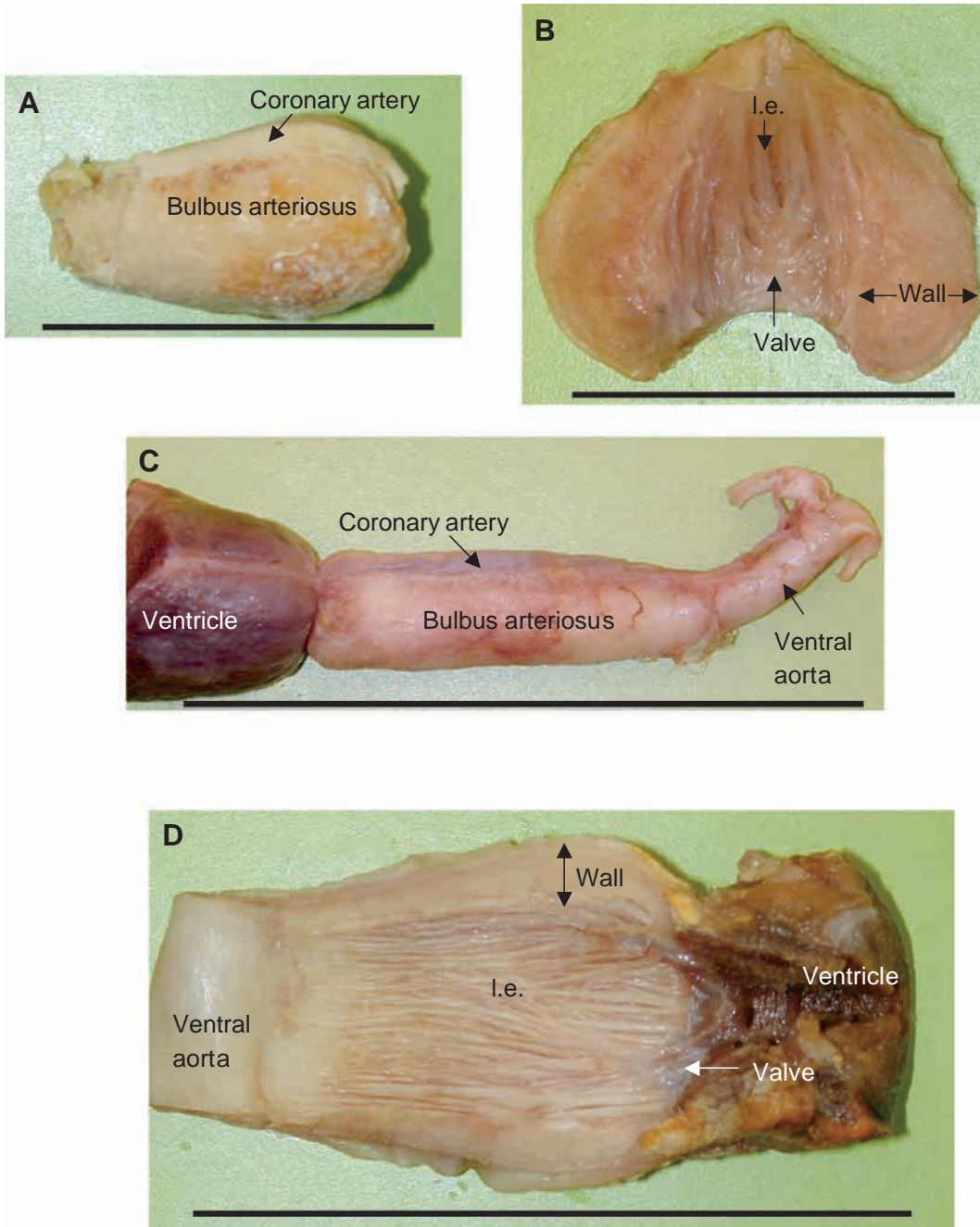The outer portion of the media (Fig. 3C) has a thick layer of

Fig. 1. (A) The bulbus arteriosus from a yellowfin tuna. Scale bar, 5 cm. (B) A yellowfin tuna bulbus opened to reveal longitudinal elements (l.e.). Scale bar, 4 cm. (C) The bulbus of a blue marlin. Scale bar, 10 cm. (D) The bulbus of a blue marlin cut open to reveal the l.e. Scale bar, 10 cm.

circumferential elastin fibres (cf), with the long axes of the fibres obvious in this transverse section. When moving from the adventitia to the lumen, an abrupt transition to longitudinal fibres (lf) occurs, marking the transition between the inner and outer media. The long axes of these elastin fibres cannot be seen; instead, the longitudinal fibres show up as small circles, the result of being sectioned transversely. The longitudinal orientation of elastin fibres is maintained throughout the longitudinal elements (Fig. 3D). However, to the right of the longitudinal element is an attached structure with neither longitudinal nor circumferential fibres. This is a radial element (re) attaching the longitudinal element to the wall.

While the majority of adventitial collagen fibres (Fig. 4A) occur in large longitudinally arranged bundles (lf), there are also smaller bundles that run circumferentially (cf). The wavy circumferential fibre bundles appear to be relatively short. Elastin and smooth muscle make up the majority of the media (Fig. 4B). Very little collagen occurs in the media or along the luminal surface (Fig. 4B). The smooth muscle cells possess a large number of plasmalemmal vesicles (arrows) surrounding much of the cell. While the bulbar elastin is not found in concentric lamellae, the fibrils do show an orientation suggesting an association with the smooth muscle cells.

Smooth muscle cells in the yellowfin bulbus are not always

sparsely distributed within the elastin (Fig. 4B). Fig. 4C shows a large number of smooth muscle cells in close proximity. The cells in this muscle layer are not attached but they do possess projections that may functionally link the cells. Layers of smooth muscle in the bulbus have been described as possessing a spiral orientation (Watson and Cobb, 1979; Yamauchi, 1980); however, it was difficult to establish an exact orientation of the muscle layer within the yellowfin tuna bulbus.

Endothelial cells modified for a secretory role are common along both the luminal surface and the longitudinal elements (Fig. 4D). These endothelial cells contain the plasmalemmal vesicles found along the margin of the membrane (arrows) as
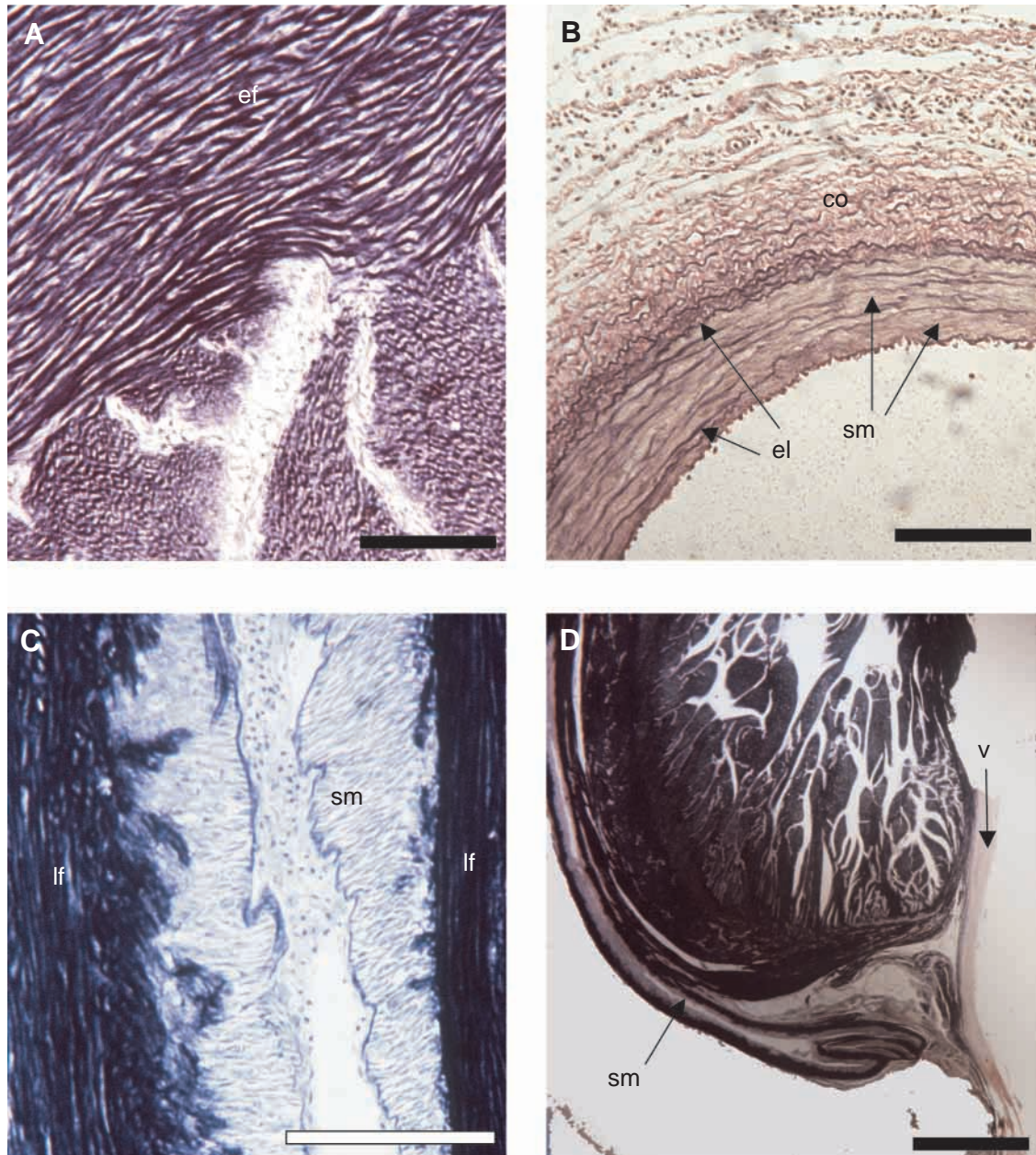

Fig. 2. Yellowfin tuna fixed at ambient pressure. (A) Transverse section through the longitudinal elements and media of the anterior bulbus. The elastin is heavily stained and shows the circumferential alignment of the elastin fibres (ef) in the media. The circumferential orientation of the elastin fibres is changed to longitudinal within the longitudinal elements. Scale bar, 100 μm. (B) Transverse section of the ventral aorta less than 1 cm anterior from the bulbus section in A. The wall of the ventral aorta is much thinner than the wall of the bulbus and has elastin lamellae (el) separated by layers of smooth muscle (sm). Collagen (co) is abundant within the adventitia. Scale bar, 100 μm. (C) Longitudinal section of the posterior bulbus. Smooth muscle occurs near the outer edge of the media, sandwiched between two layers of longitudinal elastin fibres (lf). Scale bar, 100 μm. (D) Longitudinal section of posterior bulbus. The smooth muscle layer shown in C is attached to the pocket valve (V) separating the bulbus from the ventricle. Scale bar, 1 mm. Stained with Verhoeff's elastic stain.

well as much larger vesicles (arrowheads) that are found throughout the cells.

P-V loops

After a small injection of fluid, bulbar P-V loops (Fig. 5) from both yellowfin tuna and blue marlin showed a steep initial increase in pressure that was followed by a compliant plateau phase. The yellowfin tuna bulbi were most compliant over the mean ventral aortic pressure of 12.08 ± 1.15 kPa (Jones et al.1993), while the J-shaped P-V loops of the yellowfin tuna were most compliant below the mean ventral aortic pressure (Fig. 5). In fact, most of the pressure increase in the yellowfin tuna arterial P-V loop occurred over the last 20% of volume injected. The ventral aorta of the blue marlin did not show a simple J-shaped P-V loop (Fig. 5). The slope of the curve fell before rising, resulting in two inflection points. Despite this more complex behaviour, the marlin ventral aorta possessed inflation characteristics that were comparable with those of the yellowfin tuna: large compliance at low pressures, becoming increasingly stiff over the pressure range of 10.7–21.3 kPa.
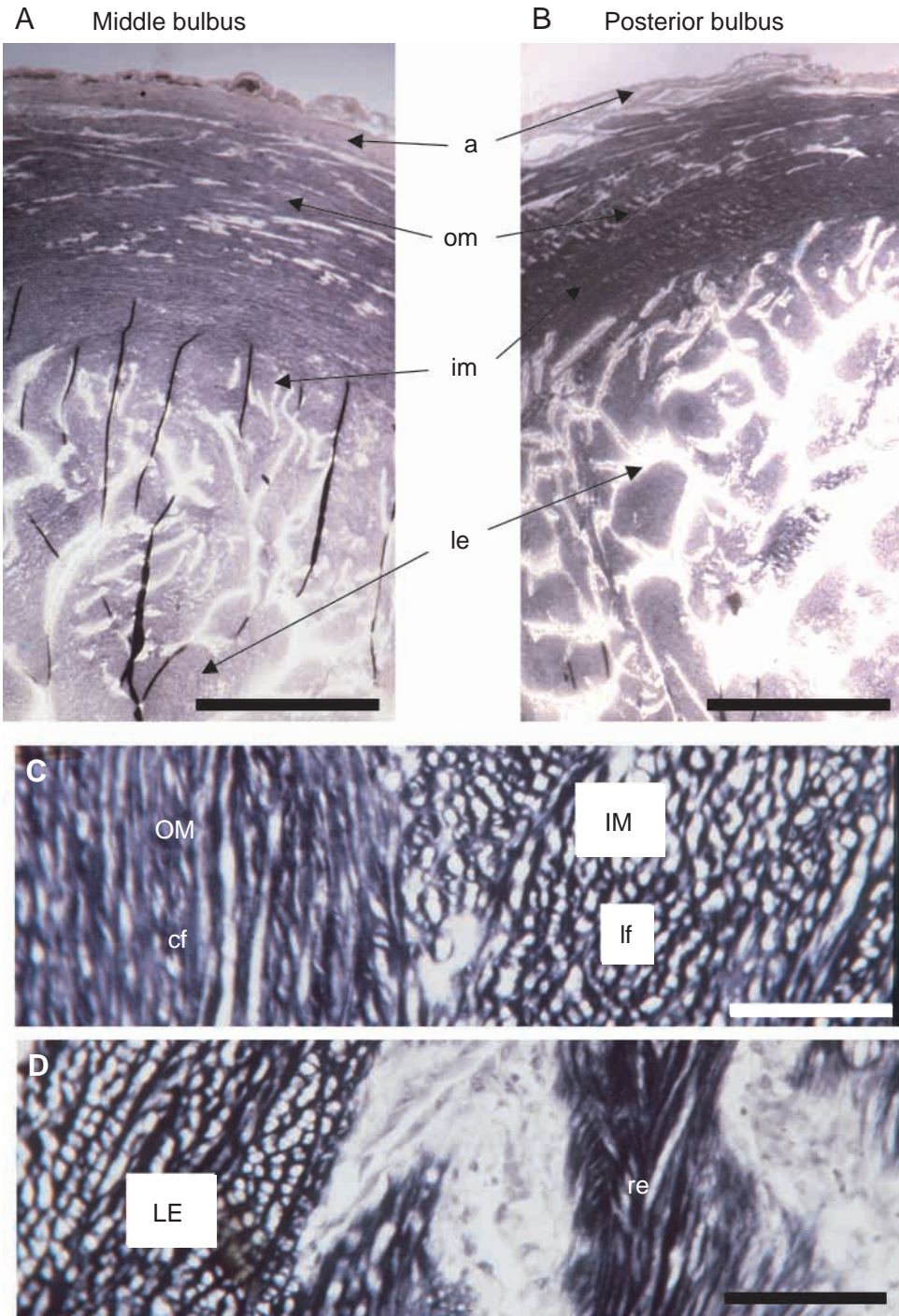

Fig. 3. Yellowfin tuna fixed at ambient pressure. All sections are transverse. (A) Middle of the bulbus. A well-defined adventitia (a), outer media (om) and inner media (im) are visible. In the dense outer media, elastin fibres are arranged circumferentially. In the inner media, elastin fibres are arranged longitudinally. The inner media contains the longitudinal elements (le). Scale bar, 500 μm. (B) Posterior bulbus. The proportions of the adventitia, outer media and inner media are changed. The outer media is half the thickness of the same layer in the middle bulbus shown in A. The size and complexity of the longitudinal elements have increased. Scale bar, 500 μm. (C) At the transition between the inner media (IM) and outer media (OM), the circumferential (cf) and longitudinal (lf) orientations of elastin fibres can be seen. The long axes of the fibres in the outer media identify them as circumferential while the small circles in the inner media show that the fibres have been transected, indicating a longitudinal orientation. Scale bar, 50 μm. (D) Longitudinal elements (LE) with the same elastin fibre pattern as the inner media. There are also radial elements (re) that attach the longitudinal elements to the lumen wall. Scale bar, 50 μm. Stained with Verhoeff's elastic stain.

On a P-V loop, the area within the loop as a percentage of the area under the inflation part of the cycle is a measure of hysteresis, or energy loss. Both the yellowfin tuna and blue marlin ventral aortae showed very little hysteresis (10.2% and 9%, respectively), indicating that they were highly resilient elastic structures.

The dorsal aorta of yellowfin tuna exhibited the continuous rise in slope with increasing volume that is of functional importance for arteries (Fig. 6). The dorsal aortae of two yellowfin tuna were parasitized by the larval cestode *Dasrynchus talismani* (Brill et al., 1987). This resulted in the dorsal aortic lumen being occluded at low pressures. As in the bulbus, the inflation behaviour of these vessels was distinctly r-shaped over much of the volume range (Fig. 6). Only at high

Fig. 4. Yellowfin tuna. All sections are transverse. (A) Electron micrograph of the collagenous adventitia. The collagen fibres are not arranged in a single direction. The majority of the fibres are arranged longitudinally (lf) but there are also bundles of circumferential fibres (cf). Scale bar, 300 nm. (B) Electron micrograph of the media. The long axes of the elastin fibrils are aligned with the long axes of the smooth muscle cells, indicating a circumferential arrangement. The smooth muscle cells possess a number of plasmalemmal vesicles along the edge of the membrane (arrow). Scale bar, 1.45 μm. (C) Electron micrograph of smooth muscle within the bulbar media. The smooth muscle cells are not always sparsely distributed within the elastin. This section shows smooth muscle cells in close proximity. The smooth muscle cells have plasmalemmal vesicles under the edge of the membrane (arrows). Scale bar, 1.55 μm. (D) Electron micrograph of a longitudinal element (le). The endothelial cells contain plasmalemmal vesicles underneath the membrane (arrow) as well as larger, electron-dense vesicles scattered throughout the cell (arrowheads). Scale bar, 1.55 μm. Stained with uranyl acetate and lead.
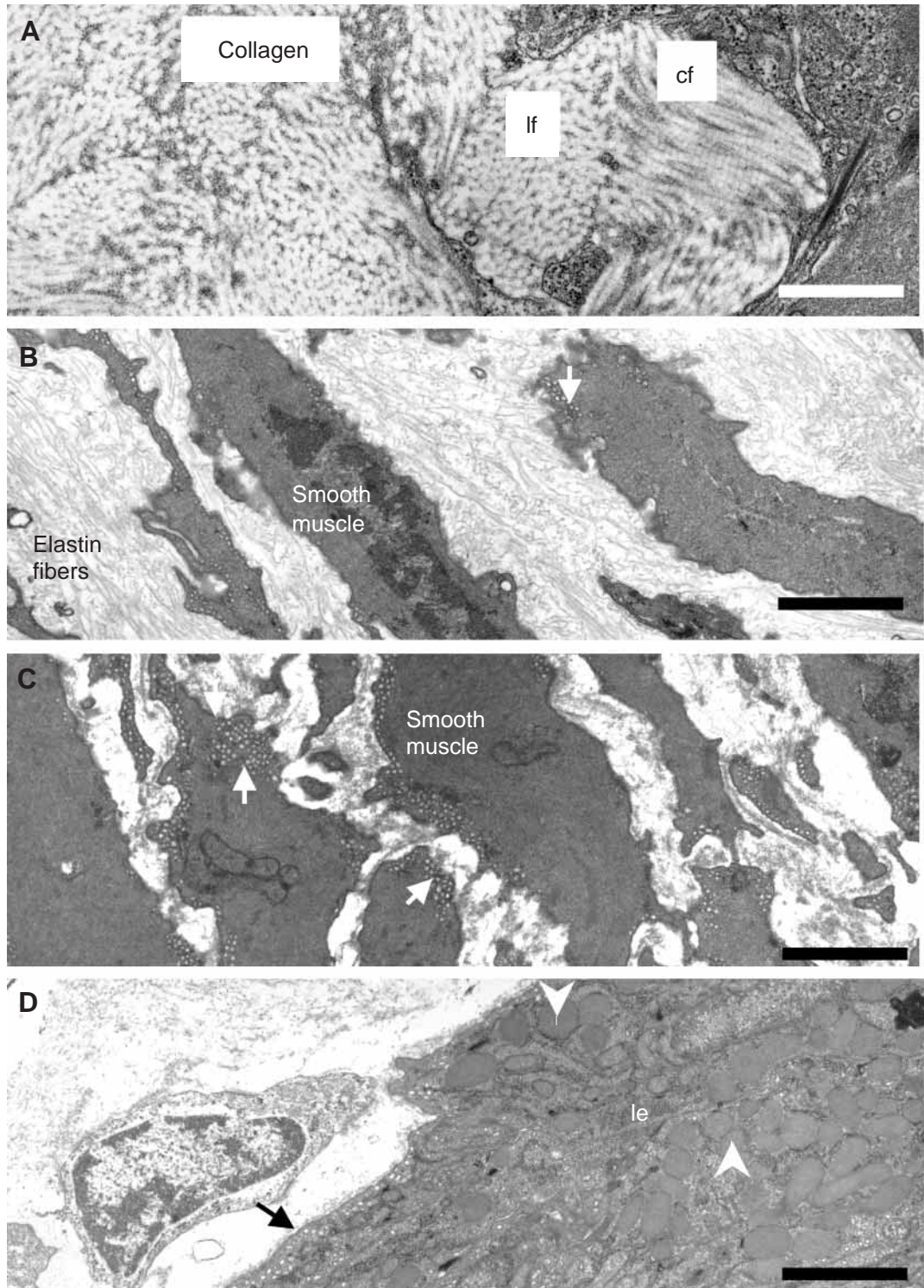
pressures did the behaviour of the parasitized and unparasitized vessels become comparable. At roughly peak systolic pressure for yellowfin tuna (Jones et al., 1993), stiffness in the parasitized aorta rapidly rose, and final pressures in both the parastized and unparasitized vessels were similar (Fig. 6).

When smooth muscle and collagen were removed or inactivated, the P-V curves of the bulbus changed. Control inflations on fresh bulbi from yellowfin tuna showed typical ſ-shaped inflation curves (Fig. 7). The addition of 10^{-5} mol l^{-1} nicardipine (a Ca^{2+} channel blocker), added to inactivate smooth muscle, decreased the magnitude of the plateau portion of the curve compared with that of the control level. Heating resulted in the bulbus becoming even more compliant, as the curve generated post-heating was lower than either the smooth muscle-blocked bulbi curves or the control bulbi curves. Repeated measures two-way ANOVA showed that the treatments had a significant effect on the P-V curves ($P<0.001$, $N=4$).

Over the same pressure range, P-V loops for inside-out blue marlin bulbi had the same shaped curves as P-V loops from normal blue marlin bulbar inflations (Fig. 5). After dissecting away the longitudinal elements, the bulbi were turned right way out and retested. Removing the longitudinal elements reduced the pressure level of the plateau (Fig. 8); however, the curve remained ſ-shaped. When the inner media was also removed and the bulbus was reinflated in its correct morphology, the curve changed drastically, with the initial slope falling 20-fold. The discrepancy in initial slopes resulted in a large difference in the pressures reached at a given volume. An inflation of 4 ml resulted in a pressure increase of approximately 1.33 kPa in the dissected bulbus, while the control curve showed a pressure of almost 10.7 kPa. When the volume in the dissected bulbus was increased from 6 ml to 8 ml of fluid, the slope rose rapidly, resulting in a pressure of 14.7 kPa (Fig. 8). The ſ-shaped inflation curve of the bulbus became J-shaped. All bulbi tested in this fashion behaved similarly.

Stress–strain experiments

Loops of the adventitia and outer media subjected to uniaxial extensions had J-shaped stress–strain and modulus–strain
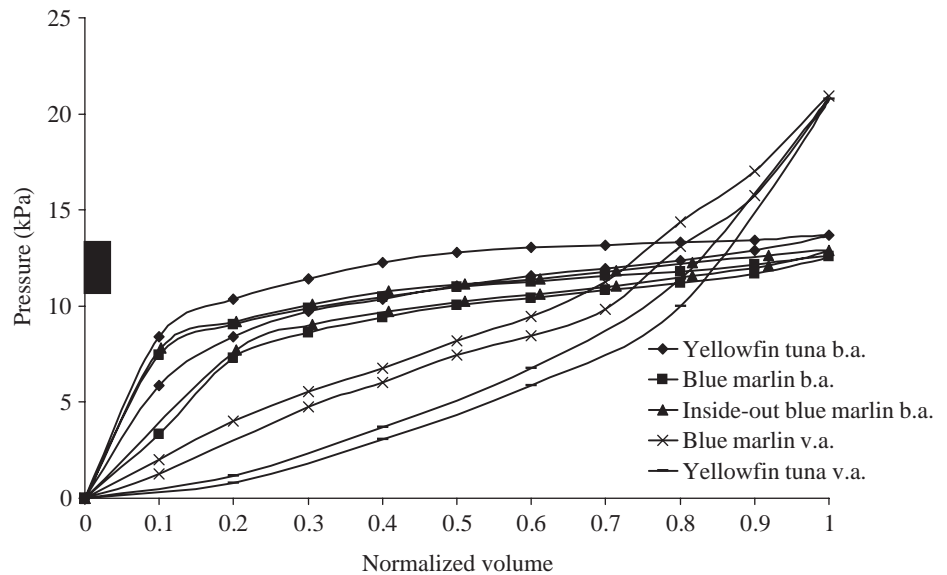

Fig. 5. Representative P-V loops from a yellowfin tuna bulbus arteriosus (b.a.), a yellowfin tuna ventral aorta (v.a.), a blue marlin bulbus arteriosus, an inside-out blue marlin bulbus arteriosus and a blue marlin ventral aorta. The bar on the *y*-axis represents the physiological pressure range for yellowfin tuna. Pressure range from Jones et al. (1993).
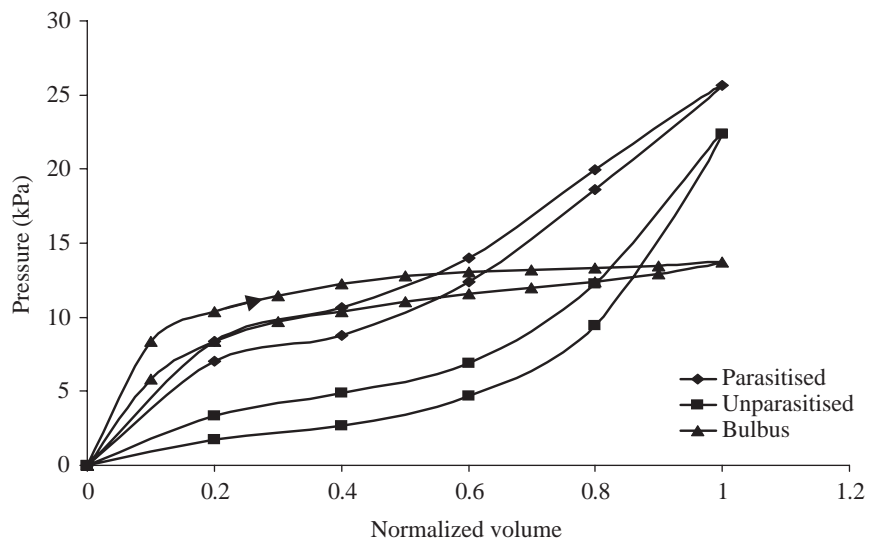

Fig. 6. Yellowfin tuna. Representative P-V loops from a parasitized dorsal aorta, an unparasitized dorsal aorta and a bulbus arteriosus.

curves; however, at strains greater than one, the adventitial layer generated higher stresses (Fig. 9A) and was much stiffer (Fig. 9B) than the outer medial layer. At a strain of 1.2, the adventitial level had a modulus of 1900 kPa, while the outer medial layer had a modulus of 180 kPa. Despite this large difference in stress and stiffness at strains above one, at strains below one the mechanical properties were similar.

While the adventitia broke at a strain of 1.25, the outer media reached strains of over 1.7. This large difference in breaking strains is somewhat misleading, because strain is normalized to the initial length of the material being tested. Since the
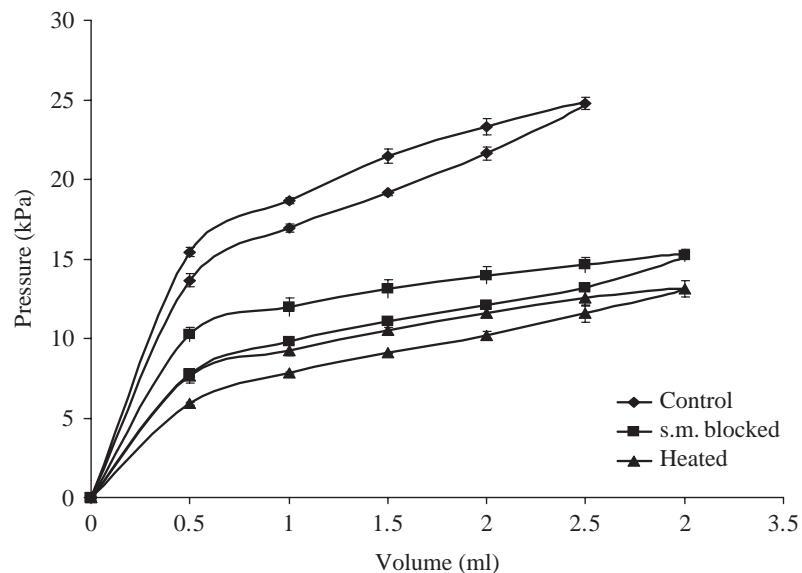
Fig. 7. Yellowfin tuna (N=4). Mean P-V loops from fresh bulbi before and after undergoing two treatments: a 10^{-5} mol l^{-1} solution of nicardipine to inactivate the smooth muscle (s.m. blocked) and a high temperature tissue bath to denature the collagen (heated). Values are means ± S.E.M.

adventitial layer had a larger initial diameter than the outer media, the absolute length at which the adventitial and medial layers broke was much closer than the breaking strains suggest.

The stress–strain curves generated from loops of tissue cut from the bulbi of yellowfin tuna (Fig. 10A) and stretched circumferentially did not have the Γ-shape characteristics of the bulbar P-V loops. Instead, the stress–strain curves had the normal J-shaped curve of many biological materials. The slope of the curve remained low until a strain of 1.2, at which point the stress rapidly increased. The modulus–strain curve (Fig. 10B) showed that the stiffness of the material rose exponentially, with the major rise beginning at a strain of 1.2. At strains below 0.8, the curves were not significantly
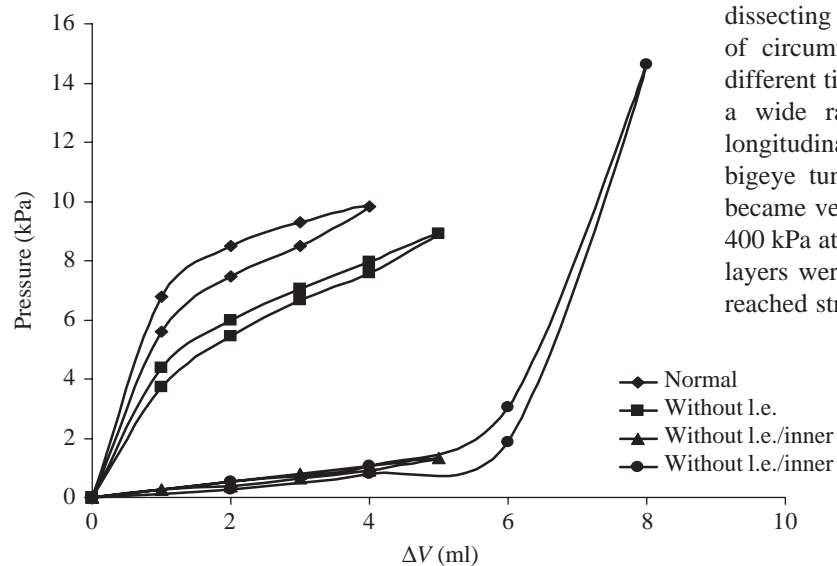
different. However, at higher strains, two-way ANOVA showed that the middle portion was significantly different (P<0.001, N=6) from the anterior and posterior portions of the bulbus; the middle section had a higher stiffness and was less extensible than both the posterior and anterior bulbar sections.

The levels of stress and modulus measured in all the portions of the bulbus, despite using the smaller value of thickness, were significantly lower than the mean value calculated for the ventral aorta (Fig. 10C). Shadwick (1999), using vessel inflations rather than uniaxial extensions, found a similar value for the elastic modulus of yellowfin tuna ventral aorta at mean blood pressure.

Like yellowfin tuna bulbar rings, blue marlin bulbar rings also reached high levels of strain when stretched circumferentially (Fig. 11). Unlike the yellowfin tuna, however, there was no difference between the different segments with regard to the values of stress or modulus (Fig. 11A,B). At a strain of 1.2 (the largest strain at which there were data for all three segments) there was no significant difference between the values of stress or modulus. The marlin ventral aorta was stiffer than the marlin bulbus (Fig. 11C); modulus values of the marlin ventral aorta were three times higher than those of the marlin bulbus at a strain of one (Fig. 11C).

Stress–strain data for the extensions of roughly rectangular bulbus segments from yellowfin and bigeye tuna are shown in Fig. 12A. The same data are plotted as modulus–strain data in Fig. 12B. The tissues obviously fell into two general groups: (1) stiff and (2) extensible. At a strain of one, the modulus for most of the tissues fell into a range that lay between 50 kPa and 100 kPa. Values gathered by stretching tissue rings (i.e. middle layer of yellowfin tuna bulbus stretched circumferentially, marked with an asterisk in Fig. 12) also fitted into this range. Despite the variability inherent in dissecting pieces of tissue away from the wall, and irrespective of circumferential or longitudinal extensions, most of the different tissues had similar values of stress and modulus over a wide range of strains. The exceptions were the two longitudinally stretched sections of bulbar outer layer from bigeye tuna. Compared with the other tissues, both pieces became very stiff at a low strain, reaching a modulus of over 400 kPa at a strain of 0.5. These longitudinally stretched outer layers were limited to strains under 0.5; the other tissues all reached strains well over one.

Fig. 8. Representative P-V loops from the bulbi of blue marlin. The bulbi have had layers of the wall dissected away. The different treatments are: normal (control); without l.e. (the longitudinal elements are removed) and without l.e./inner (the longitudinal elements and inner media are removed).

Discussion

The bulbi of yellowfin tuna and blue marlin displayed r-shaped P-V loops, while isolated bulbar rings possessed J-shaped stress–strain curves. This is paradoxical: the whole bulbus appears to have a high initial stiffness that decreases as the internal volume increases, while the material properties of isolated bulbar rings indicate that the opposite is actually true. The explanation lies in the non-linear relationship between stress and pressure as well as stress and volume. Stress (σ) is calculated as: $\sigma=(Pr)/d$, where P is pressure, r is radius and d is depth (thickness). Since thickness is expected to vary as $1/r$, stress varies as Pr^2. Strain is related to changes in r, or $V^{0.5}$. This is why a sigmoid P-V curve from a mammalian artery is transformed into a J-shaped stress–strain curve. In fact, transforming a bulbus P-V loop to stress and strain by the above approximate formulae results in J-shaped stress–strain curves.

While there is no mystery to the differences between the shapes of the bulbar P-V and stress–strain curves, the fact remains that no arterial P-V loop (sigmoid or otherwise) possesses such a steep initial rise in pressure or such a compliant plateau before the reinforcement of the collagen fibres rapidly increases the stiffness of the wall.

Qualifying the descriptions of the inflation curves as r-shaped over the physiological pressure range is obvious in the case of the yellowfin tuna. Unfortunately, we do not know the blood pressure in marlin. However, many aspects of marlin physiology are similar to those of tuna, and the available evidence suggests that marlin hearts and blood vessels are similar to those of other teleosts (Davie, 1990). The fact that tuna bulbi share their special inflation properties with *Cyprinius carpio* (Licht and Harris, 1973), *Oncorhynchus mykiss* (Priede, 1976; M. H. Braun and D. R. Jones, unpublished data) and *Oncorhynchus kitsuch* (M. H. Braun and D. R. Jones, unpublished data) suggests that, over the physiological pressure range, the r-shaped P-V loop is a feature of bulbi. For these reasons, we assumed that the r-shaped marlin inflation curve also occurs over the physiological pressure range.

The initial rise of the bulbar P-V loop is explained by the Law of Laplace, which states that $T=Pr$, where T is tension. In essence, a larger pressure is required to inflate a small cylinder than a large cylinder (assuming the two structures have similar wall thicknesses and material properties). While the external diameter of the bulbus is larger than that of the ventral aorta, the thin walls of the ventral aorta result in relatively large internal diameters at all pressures. Therefore, tension rises rapidly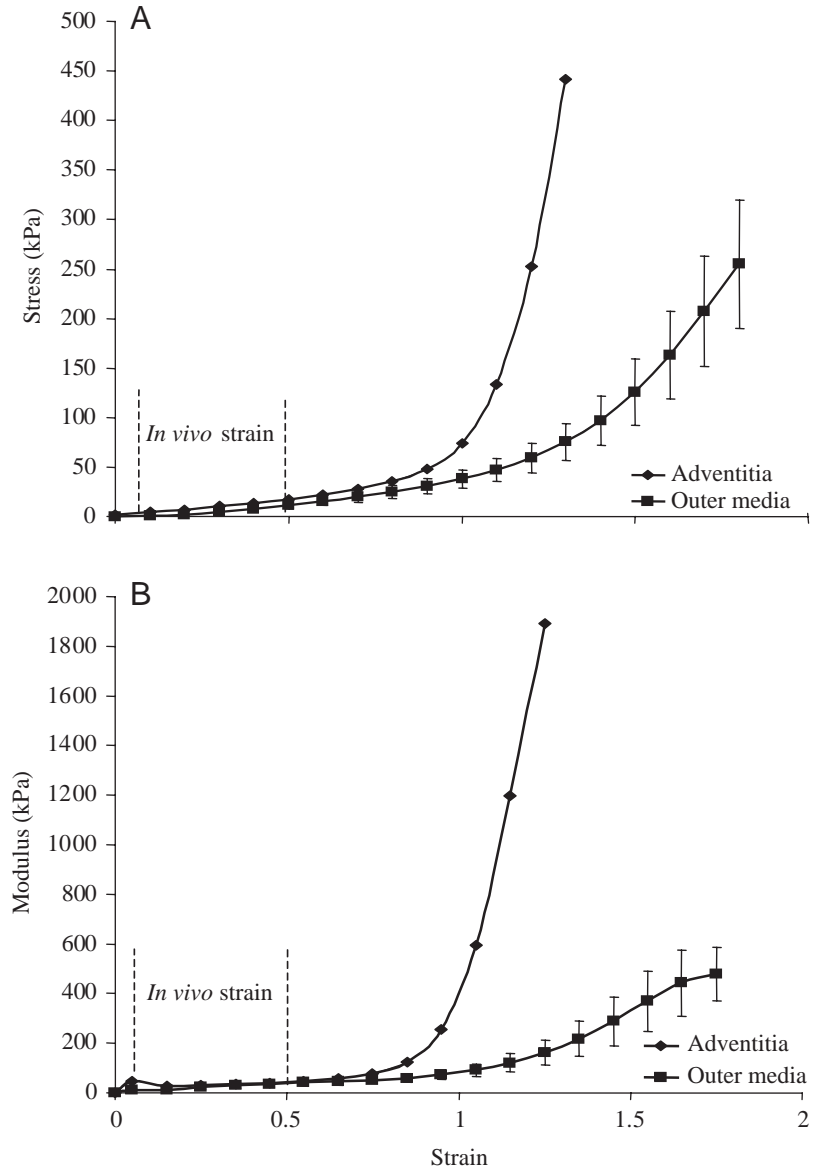 as pressure increases. In the bulbus, however, the thick wall, combined with the longitudinal elements, results in a lumen that is relatively small. In fact, when the bulbus is empty, the lumen is nearly occluded by the longitudinal elements (Fig. 13). The small bulbar lumen requires that injected volume be applied at high pressure in order to overcome the large wall tension and allow expansion.

As the longitudinal elements are pushed out to the walls and lumen radius grows (Fig. 13), wall tension decreases, and the pressure increments generated by each subsequent volume injection decline, generating the r-shaped curve. Evidence for this interaction was seen when the internal layers were removed from marlin bulbi (Fig. 8). As the effective internal radius increased, the pressure generated by the initial volume increments decreased. This resulted in a

Fig. 9. Material properties of the adventitia (*N*=1) and outer media (*N*=3) from yellowfin tuna bulbi. *In vivo* strains come from Braun et al. (2001). (A) Stress–strain curves. (B) Modulus–strain curves. Values are means ± S.E.M.

drop in the level of the plateau to the point where the inflation became J-shaped.

The yellowfin tuna dorsal aortae occluded by parastic cestodes provided a natural experiment and support our explanation of the role of the Law of Laplace in generation of the r-shaped curve. The P-V loops of normal dorsal aortae were essentially J-shaped, while, over much of the *in vivo* pressure range, the P-V loops for the parasitized aortae (despite being structurally identical to the unparasitized specimens) were distinctly r-shaped. Just as the bulbus required the initial volume to be injected at a large pressure to push the longitudinal elements against the inner wall, the parasitized dorsal aorta also developed a large pressure that would push the long thin larval cestodes aside, opening the lumen for flow. However, at large volumes, while the bulbar curve remained relatively flat, the parasitized aorta showed the same large rise in pressure as occurred in the unparasitized aorta. The bulbus is more than an occluded artery, and another mechanism is required to explain the compliant plateau phase of the bulbar P-V loop.

The bulbus is composed primarily of elastin, with estimates of the actual amount of elastin within the bulbus ranging from 70% in salmonids (Serafini-Fracassini et al., 1978) to 90% in carp (Licht and Harris, 1973). In rainbow trout, the elastin:collagen ratio is about 14 (Serafini-Fracassini et al., 1978), compared with 1.5 in mammalian proximal aorta (McDonald, 1974). The higher the elastin:collagen ratio, the more compliant is the structure. Licht and Harris (1973) found the bulbus to be 32× more distensible than the human thoracic aorta over the same pressure range. In both yellowfin tuna and blue marlin, the bulbi had larger breaking strains and much lower moduli than the respective ventral aortae. The large extensibility and low modulus are key to the extreme compliance of the bulbus during the plateau of the P-V loop.

Unlike many fish arteries (Leknes, 1986), the design of the yellowfin tuna ventral aorta is very similar to that of the mammalian artery (Dobrin, 1978), with concentric elastic lamellae separated by layers of smooth muscle and collagen
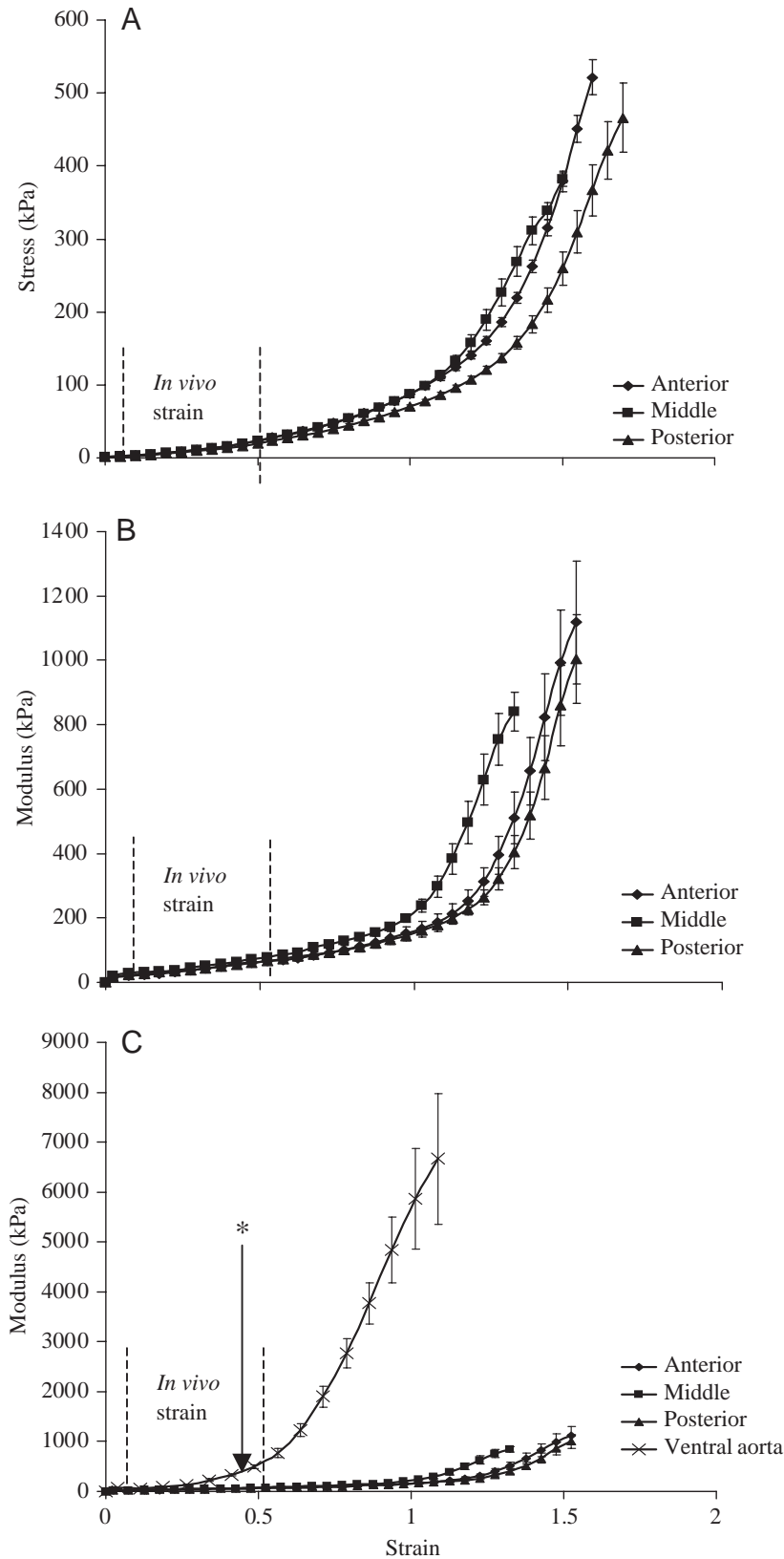
Fig. 10. Material properties of segments from the bulbus (N=6) and ventral aorta (N=3) of yellowfin tuna. *In vivo* strains come from Braun et al. (2001). (A) Stress–strain curves of the anterior, middle, and posterior portions of the bulbus. (B) Modulus–strain curves of the anterior, middle and posterior portions of the bulbus. (C) Modulus–strain curves comparing the ventral aorta to the anterior, middle and posterior portions of the bulbus. Values are means ± S.E.M. The asterisk indicates the modulus value for yellowfin tuna ventral aorta at mean physiological pressure, as calculated by Shadwick (1999) using vessel inflations.

(Fig. 2B). While this may be an adaptation to the high blood pressures of tuna, no similar adaptation has occurred within the yellowfin tuna bulbus (Figs 2A, 4B). In teleosts, bulbar elastin is found not in lamellae but in fibrils (Licht and Harris, 1973; Serafini-Fracassini et al., 1978; Benjamin et al., 1983; Icardo et al., 2000), and collagen has been largely relegated to the thin adventitia. The intimate connections between elastin and smooth muscle seen in mammalian arteries do not exist in the bulbus.

Teleost elastin, unlike its mammalian counterpart, is not found in elastic fibres composed of an amorphous elastin component and elastin-associated glycoprotein microfibrils. Elastin-associated microfibrils are extremely rare in teleost arteries (Isokawa et al., 1990), and teleost arterial elastin is almost exclusively found in a fibrillar form, a morphology shared with the bulbus. While the fibrils of elastin superficially resemble the glycoprotein microfibrils of mammalian elastic fibres, Serafini-Fracassini et al. (1978), Benjamin et al. (1983) and Isokawa et al. (1988) have demonstrated, using elastases, elastin stains and molecular analyses, that the fibrils are elastin.

The benefits of the fibrillar design of bulbar elastin can be seen in the considerable radial expansion that the bulbus experiences during each heart beat. Benjamin et al. (1983) have suggested that lamellar sheets would be unable to manage the large-scale length changes required. Either the sheets would tear at high strains or the folding necessary at low strains would disrupt the structure of the bulbar wall. However, these problems suggested by Benjamin et al. (1983) could be remedied by relatively minor lamellar modifications. Longer lamellae, which would require a larger extension before becoming taut, would eliminate possible damage at large strains. Packing the lamellae at low strains would likely be inconsequential, as the inner bulbar wall is already thrown into numerous folds and trabeculae. We hypothesize that the fibrillar design of the bulbus does not combat the dangers of large expansions; it lowers the modulus of the material.

It is unlikely that the low modulus of the bulbus is due merely to the gross structure of the elastin fibrils. Teleost elastin is chemically distinct from other elastin variants (Serafini-Fracassini et al., 1978; Spina et al., 1979; Sage, 1982; Chow et al., 1989), with a decreased hydrophobic index due to an increase in polar amino acids. As much of the recoil in elastin is driven by hydrophobic interactions, this may result in a lower elastic modulus. Bulbar elastin dissolves under conditions the ventral aortic elastin can withstand (Licht and Harris, 1973), suggesting that the bulbar variety is even less hydrophobic than ventral aortic elastin and may be the result of a different gene product.

In most arteries, it is the close association of elastin with collagen that provides the exponential rise in
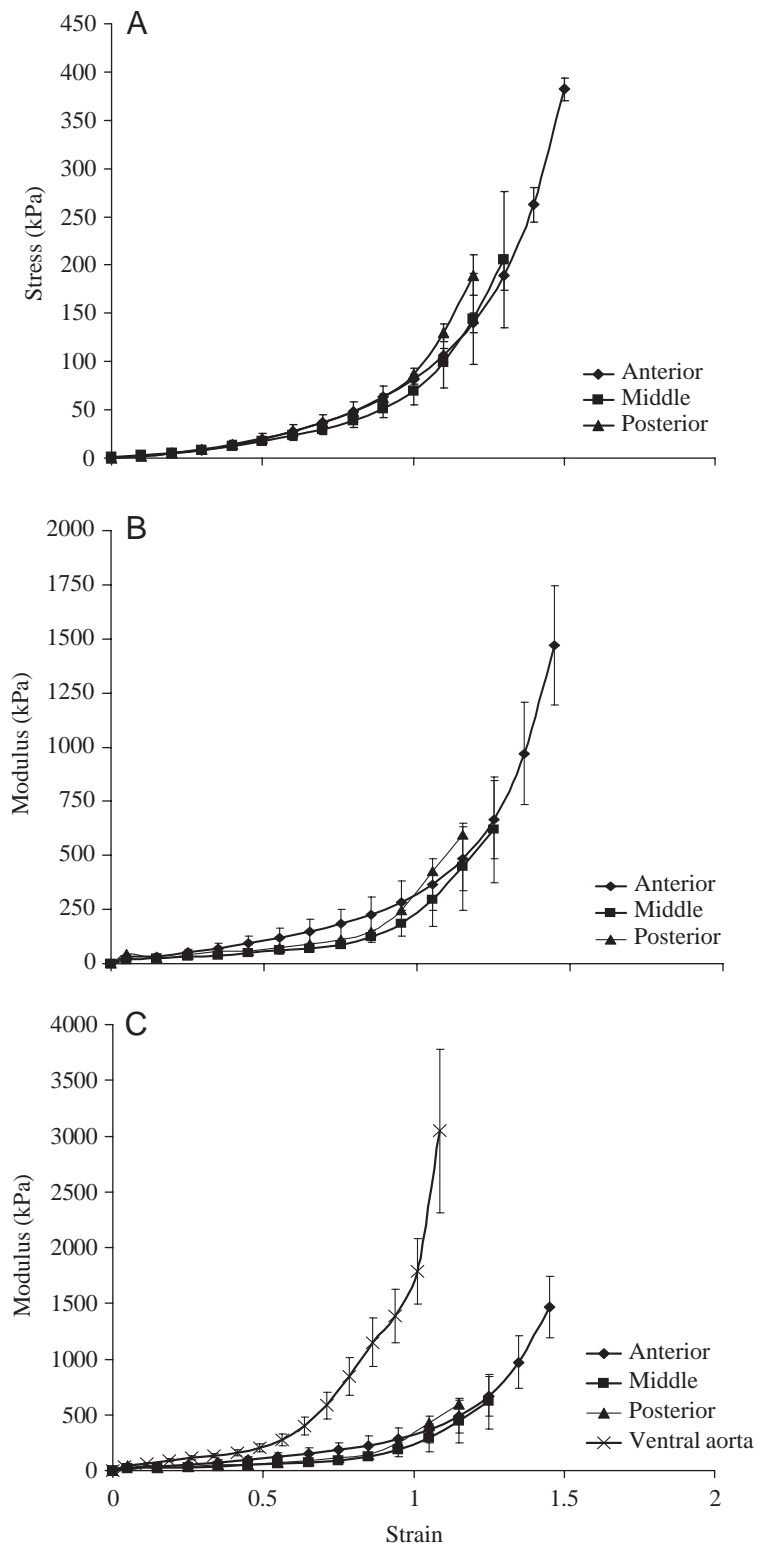
Fig. 11. Material properties of different segments from the bulbus (*N*=4) and ventral aorta (*N*=3) of blue marlin. (A) Stress–strain curves and (B) modulus–strain curves of the anterior, middle and posterior portions of the bulbus. (C) Modulus–strain curves comparing the ventral aorta to the anterior, middle and posterior portions of the bulbus. Values are means ± S.E.M.

stiffness as inflation increases. Much of the bulbar collagen is confined to the adventitia, a loose, fibrous layer that is not as dense as the outer media (Fig. 4A). Benjamin et al. (1983),

Raso (1993) and Icardo et al. (1999a,b, 2000) have suggested that the adventitia is primarily responsible for limiting the radial distension of the bulbus. However, the adventitia has a modulus that is similar to that of the outer media at strains below one. At these levels, the outer medial layer actually bears more of the load in the wall than the adventitia does, due to differences in their respective wall thicknesses.

Very large strains, at which the adventitia would bear the majority of the load, would result in the third stage of a sigmoid inflation curve: a rapid increase in pressure with increasing volume. This feature of the bulbus was suggested by the exponential rise in stiffness as tissue samples encompassing the entire wall were subjected to large strains (Figs 9–12). The sharp rise in pressure was also seen during inflations of bulbi with much of the wall removed (Fig. 8). Ordinarily, the thick media is the primary layer resisting bulbar expansion, while the thin adventitia is only recruited at large strains (>1). By removing the media, the adventitia was the only layer resisting the increasing strain and expanded much more than it ordinarily would at any given pressure. This resulted in the adventitia becoming taut at a low ΔV. While the tensile tests (Figs 9–12) and modified inflations (Fig. 8) show that the bulbus is capable of a final increase in stiffness, they also show that, for this to occur in a bulbar inflation, extremely large volumes (and pressures) would be required. *In vivo*, the constraints of the stiff pericardium would limit the amount of bulbar expansion, and the chances of the bulbus reaching a large enough strain to recruit the adventitia are small. However, by limiting bulbar expansion, the pericardium itself may cause the final rise in pressure.

The majority of adventitial collagen is actually longitudinally oriented, preventing longitudinal rather than radial expansion (Fig. 4A). Compared with the other tissues, the adventitia of bigeye tuna bulbus only became very stiff at a
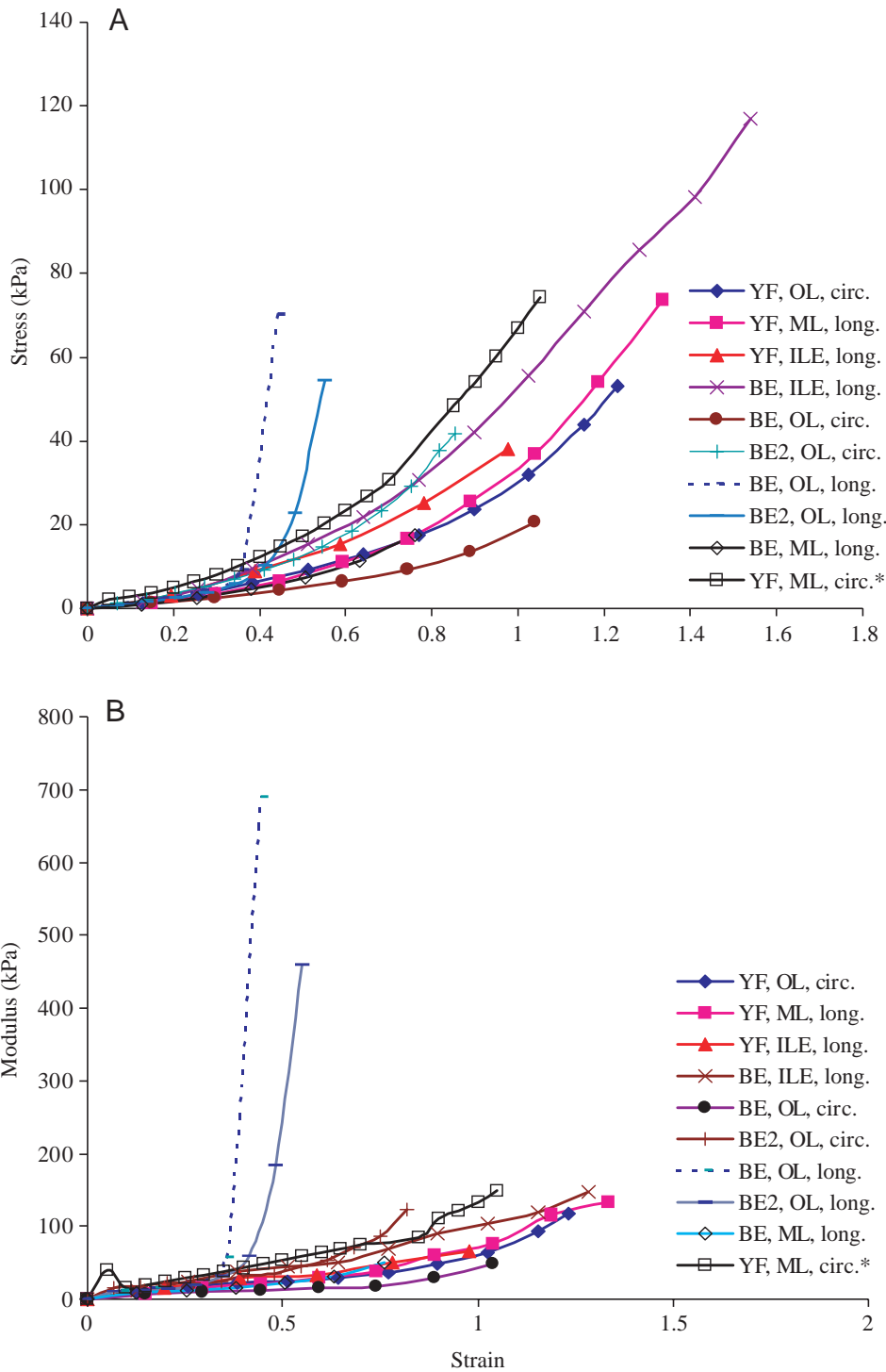
Fig. 12. Material properties of the bulbi of yellowfin and bigeye tuna. (A) Stress–strain curves. (B) Modulus–strain curves. The following rectangular tissue samples were stretched using a micromanipulator: YF, yellowfin tuna; BE, bigeye tuna; ML, segment of the middle layer; ILE, segment of longitudinal element; OL, segment of the outer layer; circ., stretched circumferentially; long., stretched longitudinally. The asterisk represents a tissue sample that was stretched as a loop using the custom-built stretching machine.

Low pressure   High pressure
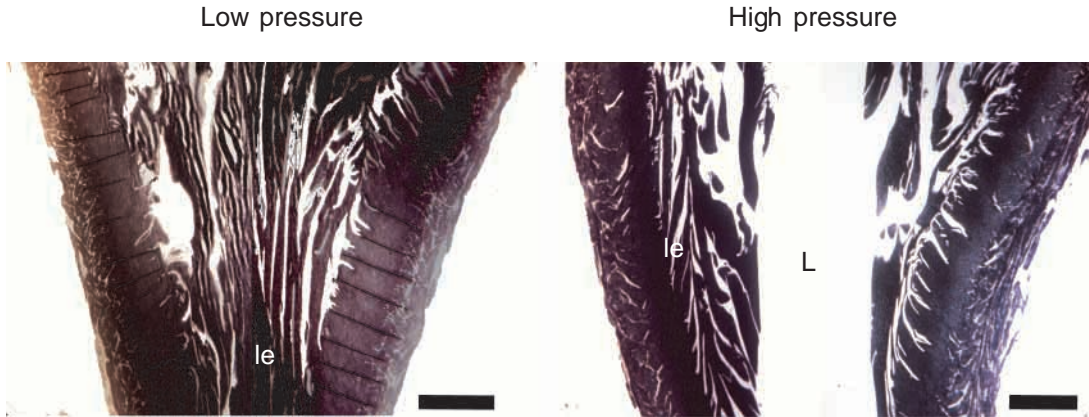
Fig. 13. Longitudinal sections from the bulbus arteriosus of yellowfin tuna. The high pressure section was fixed at 14.7 kPa. The longitudinal elements (le) are pushed to the side of the lumen (L) at high pressure. Scale bar, 1 mm. Stained with Verhoeff's elastic stain.

low strain when stretched in the longitudinal direction (Fig. 12). The outer layer was limited to a strain of 0.5 when stretched longitudinally, while all other tissues reached strains greater than one. The maximum *in vivo* longitudinal strain reached by yellowfin tuna bulbi has been measured at 0.48 (Braun et al., 2003).

Therefore, the answer to the question about the bulbus' extensibility on the plateau of the curve is multifaceted. The arrangement of the collagen and the structure and chemical nature of the bulbar elastin all combine to allow large volume changes within the bulbus for small pressure changes during the plateau phase of the inflation.

While elastin and collagen are important, smooth muscle function in the bulbus is not insignificant. It is innervated (Watson and Cobb, 1979), responds to a wide variety of pharmacological and environmental stimuli by increasing or decreasing the bulbar distensibility (Farrell, 1979) and causes large changes in the inflation characteristics of the bulbus when it is prevented from contracting (Fig. 7): a larger change than that due to the denaturation of the bulbar collagen. While an extremely compliant vessel would limit the fish's ability to increase blood pressure when needed, smooth muscle appears able to adjust the stiffness of bulbi to match the demands of the fish. With smooth muscle, the bulbar properties can be 'tuned' to the situation at hand. While this role of smooth muscle is in contrast to previous speculation (Licht and Harris, 1973) that bulbar smooth muscle serves merely to produce elastin, the numerous plasmalemmal vesicles seen in yellowfin tuna smooth muscle (Fig. 4B,C) do suggest a secretory role.

The bulbus seems to have been designed to allow maximal expansion, with many of the safeguards against rupture found in arteries either lacking or reduced and with much of the remaining collagen arranged to limit longitudinal rather than circumferential expansion. This suggests that the bulbus is at risk of rupture; however, *in vivo*, the bulbus is enclosed by the fibrous pericardium, limiting circumferential expansion. The longitudinally arranged collagen is vital as the bulbus is only tethered at its distal end, and unchecked longitudinal expansion would interfere with cardiac function by kinking the ventral aorta and occluding the lumen.

The function of longitudinal elements in teleosts has never been properly explained. Priede (1976) contended that they acted as struts, supporting the bulbus wall during inflation cycles. Due to the thick bulbar wall, the inner layers are subjected to much larger strains than are the outer layers. Since the longitudinal elements do not undergo the same circumferential strains, the problem of strain distribution would be solved. Fig. 12 shows that the longitudinal elements have no greater stiffness or strength than the other materials in the wall. Thin, extensible, 'floppy' struts would be of little use in a supportive role, and unequal strain distribution through the thick wall is not a problem because the bulbus is not made of an isotropic material. Different amounts and orientations of elastin, collagen and smooth muscle in the adventitia and media generate a host of material properties. Even though the media experiences a larger absolute strain than the adventitia during bulbar expansion, the media has a higher breaking strain than the adventitia (Fig. 9). Designing the bulbus with anisotropic properties, specifically a higher breaking strain for the media, prevents early failure.

The bulbi of all fish are subject to large expansions, while longitudinal elements seem to be limited to high-performance fish. Any functional explanation of the longitudinal elements would need to take into account the biology of the species possessing them. All these fish (including tuna, marlin, sailfish, trout and salmon) have a suite of adaptations allowing them to maintain aerobic activity for far longer than the average teleost, and the longitudinal elements may also be an adaptation towards a high-performance lifestyle. When the longitudinal elements are removed, the magnitude of the pressure generated on initial inflation drops (Fig. 8). When the longitudinal elements fill up the lumen at the end of diastole (Fig. 13), the bulbus requires a higher pressure for initial inflation. Longitudinal elements may be necessary to ensure that the higher pressure requirements of those fish that possess them are met. During diastole, the bulbus bears down on the contained blood, maintaining flow across the gills. During cardiac ejection, the compliant, easily stretched longitudinal elements are pushed out to the sides of the vessel wall, greatly increasing lumen size and allowing blood to pass freely.